Electronic Supplementary Material (ESI) for Journal of Materials Chemistry B.

Supporting Information

Fabrication of anti-freezing and self-healing nanocomposite hydrogels based on phytic acid and cellulose nanocrystals for high strain sensing applications

Dongqi Yue, Shaoning Shi, Hou Chen*, Liangjiu Bai*, Wenxiang Wang, Huawei Yang, Lixia Yang, Donglei Wei

School of Chemistry and Materials Science, Ludong University, Key Laboratory of High Performance and Functional Polymer in the Universities of Shandong Province, Collaborative Innovation Center of Shandong Province for High Performance Fibers and Their Composites, Yantai 264025, China.

*Corresponding authors: E-mail address: chenhou@ldu.edu.cn (H. Chen) and bailiangjiu@ldu.edu.cn (L. J. Bai)

Experimental

Materials

Pyrrole (99.0%, Energy Chemical). Microcrystalline cellulose (MCC, ≥99.0%, Zhengzhou Alfa Chemical Co., Ltd.). Phytic acid (PA, 70% in H_2O, Aladdin Biological Technology Co., Ltd.). Ferric chloride hexahydrate ($FeCl_3 \cdot 6H_2O$, ≥99.0%, Sinopharm Chemical Reagent Co., Ltd.). Sulphuric acid (H_2SO_4, ≥95.0%, Yantai Far Eastern Fine Chemical Co., Ltd.). Poly(diallyldimethylammonium chloride) (PDDA, M_w = 100,000-200,000 g/mol, Macklin Biochemical Co., Ltd.). Poly(vinyl alcohol) (PVA, M_w = 75000 g/mol, Energy Chemical).

Mechanical properties and self-healing ability of the hydrogels

Tensile experiment was obtained with LDW-5 microcomputer control electronic universal material testing machine (Songdun, Shanghai). The hydrogel sample was cut into 50 × 4 × 1 mm dumbbell shape to evaluate the mechanical properties. The self-healing rate of hydrogel could be obtained by eq. (1):

$$Self-healing\ efficiency(\%) = \frac{\sigma'}{\sigma} \times 100\% \qquad (1)$$

where σ was the fracture stress of the original hydrogel and σ' was the fracture stress of the repaired hydrogel.

Evaluation of swelling properties

The same mass of nanocomposite hydrogel was immersed in distilled water and the change in weight was recorded by removing the excess water from the surface after some time. The swelling ratio (SR) of the hydrogel was obtained from eq. (2):

$$SR(\%) = \frac{(W_t - W_0)}{W_0} \times 100\% \quad (2)$$

where W_0 was the original weight of hydrogels, W_t was the weight of the hydrogels at a certain time.

Assembly and characterization of the hydrogel strain sensors

The hydrogel was cut into strips of 40 × 15 × 1 mm size as test samples. Two conductive adhesive tapes were attached to both ends of the hydrogel sample and connected to a digital multimeter (Model 2400, USA) to assemble the hydrogel strain sensor. Hydrogels were attached to different parts of the body to monitor human movement. The gauge factor (GF) of the hydrogels was calculated by eq. (3):

$$GF = \frac{(R - R_0)/R_0}{\varepsilon} \quad (3)$$

where ε was the applied strain, and R and R_0 represented the real-time resistance and the initial resistance, respectively.

Characterization and methods

Scanning Electron Microscope (SEM) images were presented on the microscope of Hitachi SU-8010. Fourier Transform infrared spectroscopy (FT-IR) were measured via Nicolet iS50. X-ray photoelectron spectroscopy (XPS) were obtained with an electron spectrometer (ESCALAB Xi+). The thermogravimetric analysis (TGA) was measured on TGA 4000 (Perkin Elmer, USA) analyzer at a heating rate of 10 °C/min in the temperature range between 50 and 700 °C under an N_2 atmosphere. X-ray diffraction (XRD) was performed on diffractometer (Bruker D8). Tensile experiment was obtained with LDW-5 microcomputer control electronic universal material testing machine

(Songdun, Shanghai). The self-healing process of hydrogels were performed on the DMM-300C metallurgical microscope. The freezing resistance of hydrogels were measured using differential scanning calorimetry (DSC, Netzsch 204F1). Testing range was fulfilled from 20 to -70 °C at a rate of 10 K/min under a nitrogen atmosphere. Research on sensing performance were enforced on Keithley analyzer (Model 2400, USA).

Table S1. The comparison of anti-freezing, self-healing and mechanical properties of various anti-freezing hydrogels.

Component	Anti-freezing agents	Low-temperature Operation (°C)	Mechanical Properties (strain)	Self-healing efficiency	Refs.
PVA/LS/LiCl/EG	LiCl/EG	-18	-	-	[S1]
PAA/ISP-Ca	ISPs/$CaCl_2$	-20	890%	-	[S2]
Cellulose based hydrogels	$ZnCl_2$/$CaCl_2$ /Glycerol	-70	120%	-	[S3]
PAM/SA/TOCNs /$CaCl_2$	DMSO/$CaCl_2$	-20	661%	-	[S4]
PGT hydrogel	$AlCl_3$/Glycerol	-14	1200%	-	[S5]
DSI-skin	$AlCl_3$	-15	170%	85.0%	[S6]
Gel-TA@CNCs-L	L-proline/$FeCl_3$	-15	550%	80.8%	[S7]
PVA/EG/TA/$CaCl_2$	EG/$CaCl_2$	− 32	606.8%	89.24%	[S8]
GAPS hydrogel	Maltose/Trehalose	−28.9	329%	88.4 %	[S9]
PVA/PDDA /CNCs-g-PPy/PA	PA	-15	851.8%	92.9%	This work

Table S2. The experimental ingredients of hydrogels and comparison of mechanical properties with various mass of PA and CNCs-*g*-PPy.

Component	PA content (wt%)	CNCs-*g*-PPy content (mg)	PVA (g)	PDDA (g)	Stress (KPa)	Strain (%)
PA-1	30	4	0.8	0.2	188.8	705.6
PA-2	35	4	0.8	0.2	296.5	790.8
PA-3	40	4	0.8	0.2	143.7	785.9
PA-4	45	4	0.8	0.2	81.6	639.4
CNCs-*g*-PPy-1	40	0	0.8	0.2	122.5	780.7
CNCs-*g*-PPy-2	40	4	0.8	0.2	144.0	785.9
CNCs-*g*-PPy-3	40	8	0.8	0.2	162.9	850.0

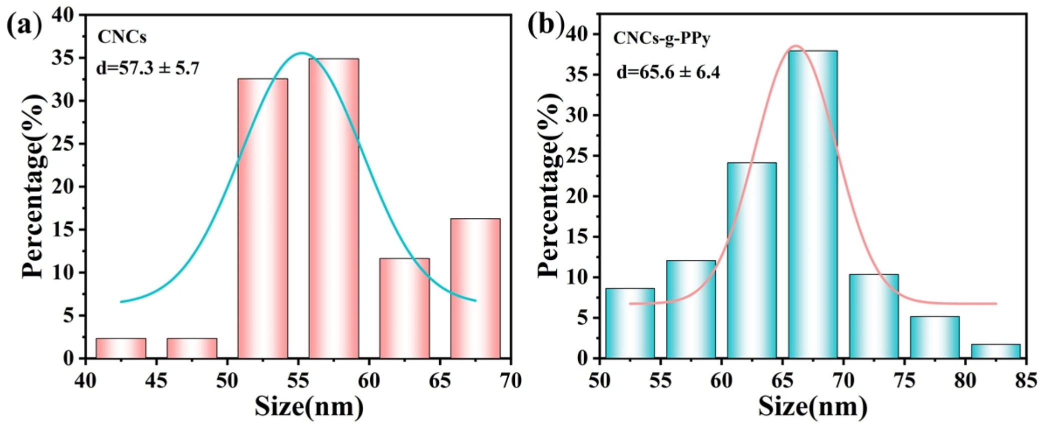

Fig. S1. (a) Width analysis of CNCs and (b) CNCs-*g*-PPy.

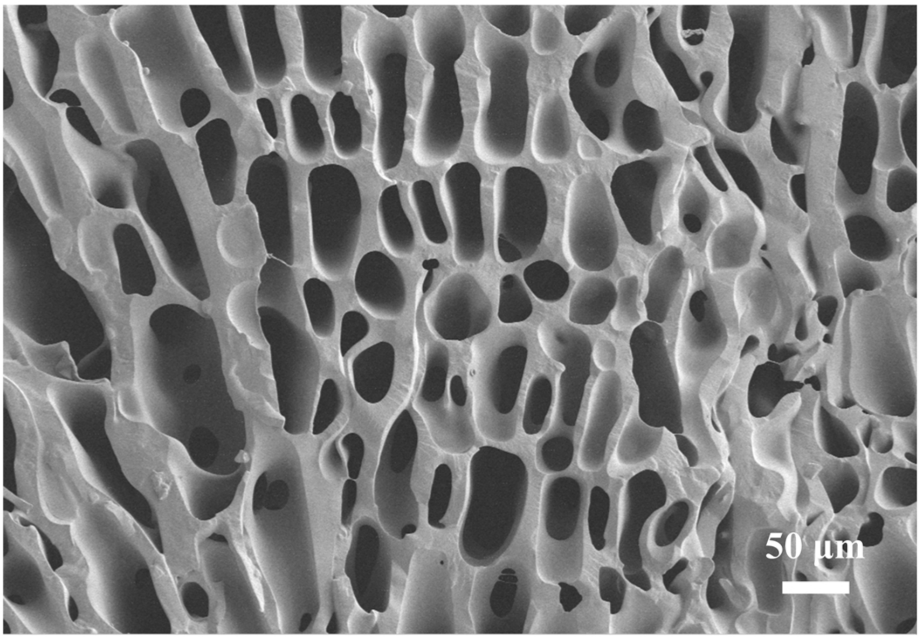

Fig. S2. SEM cross-sectional images of hydrogels.

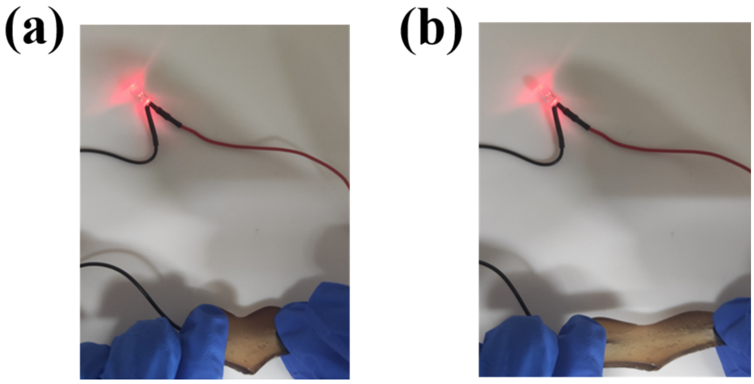

Fig. S3. Brightness variations of LED lamps under different strains.

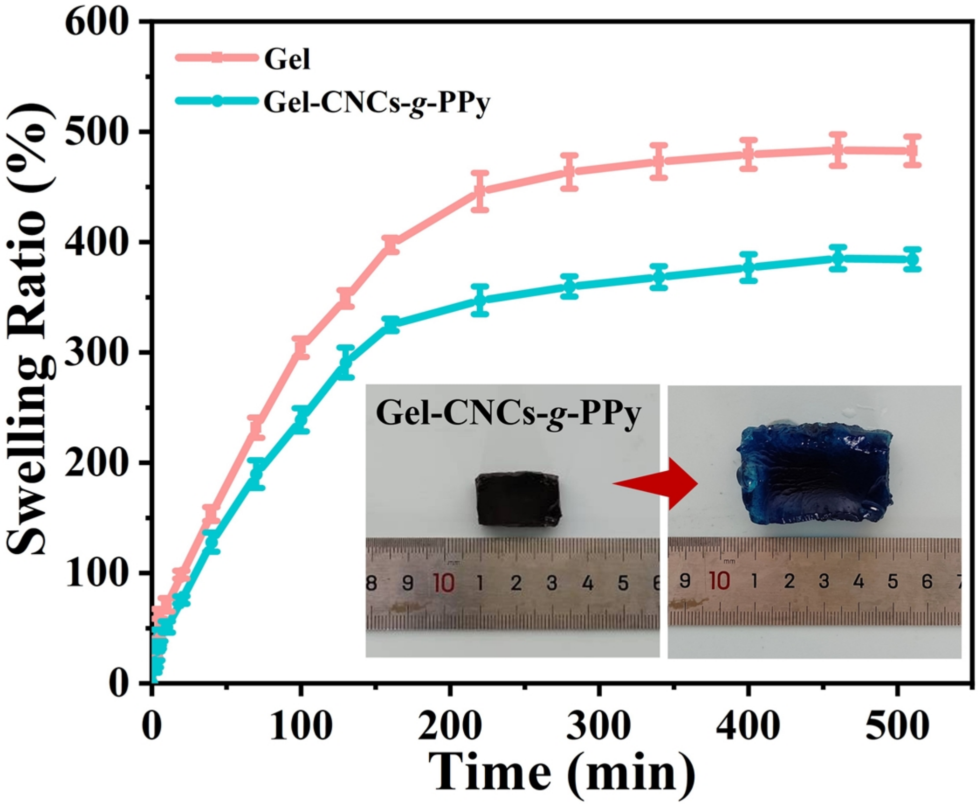

Fig. S4. Evaluation of the swelling properties of hydrogels.

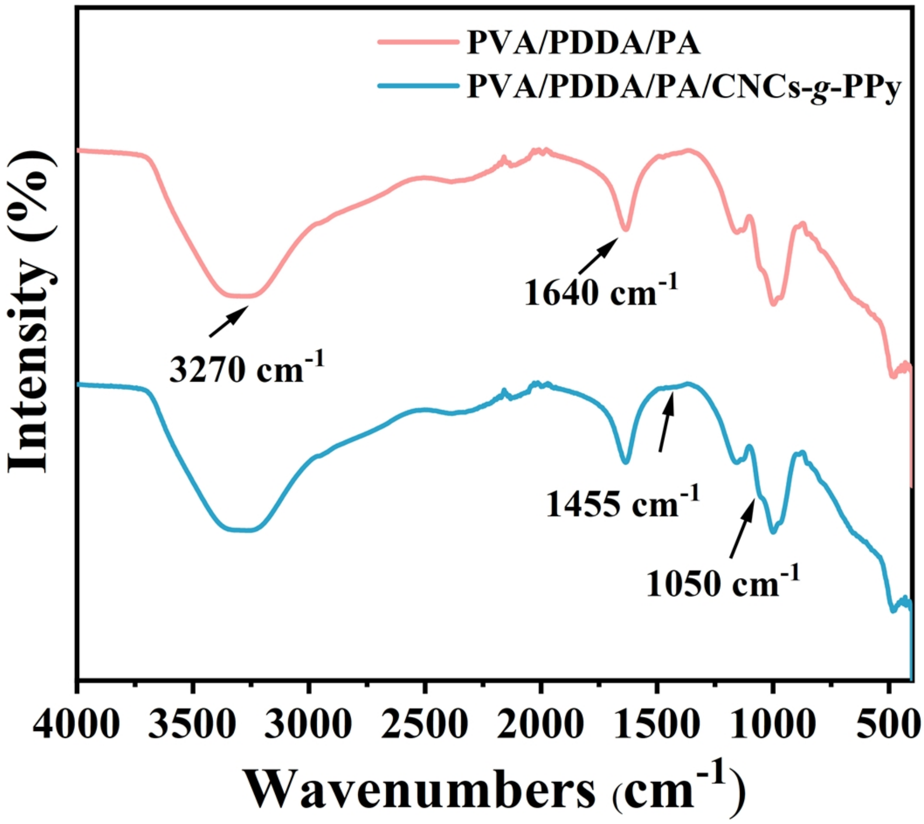

Fig. S5. FT-IR spectra of the PVA/PDDA/PA and PVA/PDDA/PA/CNCs-g-PPy.

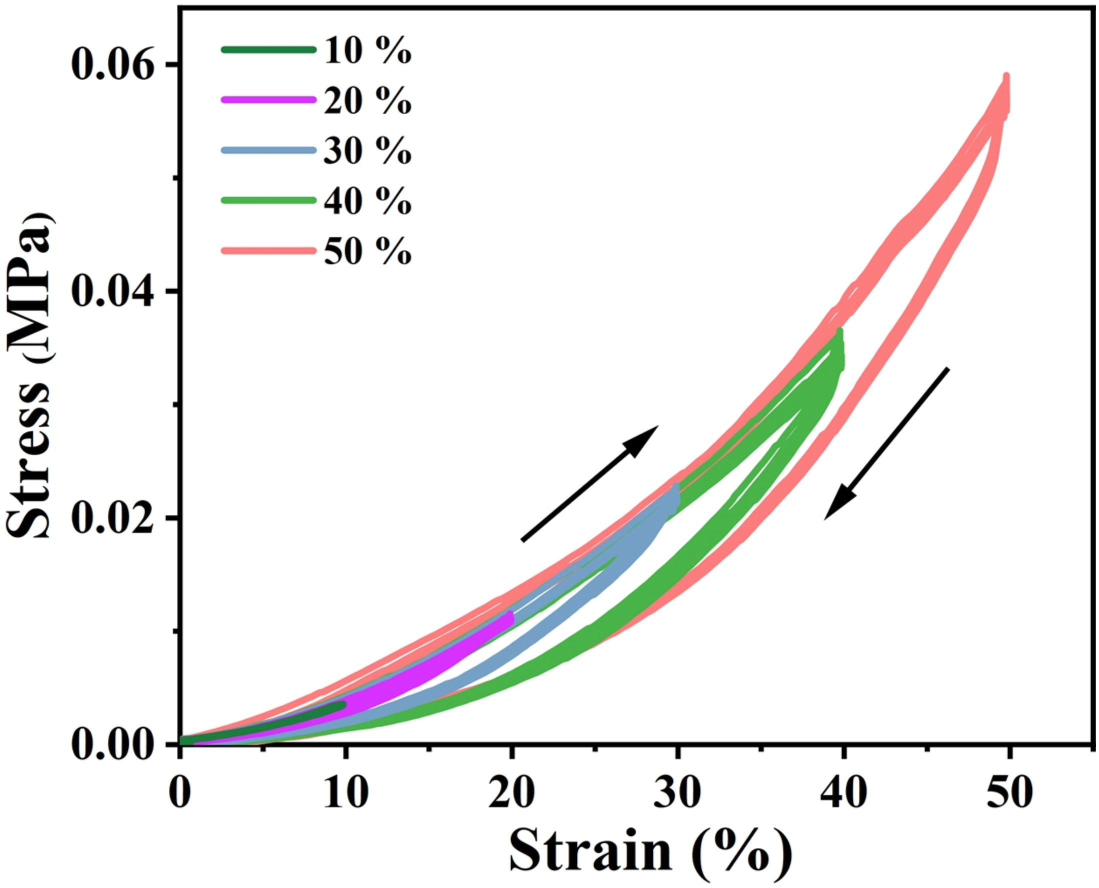

Fig. S6. Cyclic compression curves of hydrogels at 10%, 20%, 30%, 40% and 50% strain.

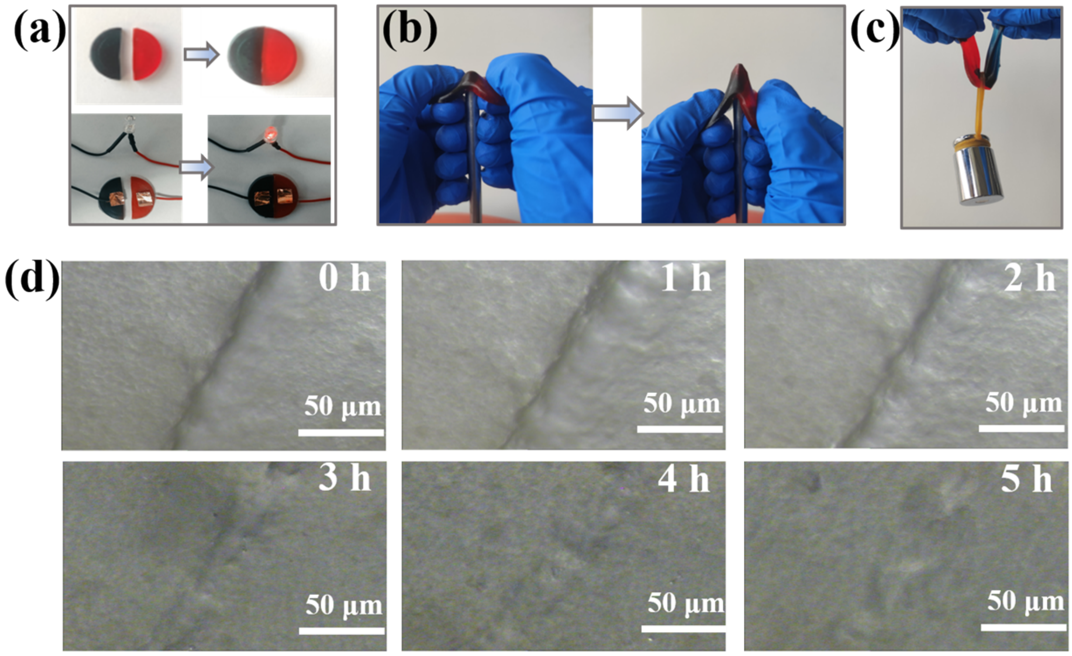

Fig. S7. Macroscopic images of healing process at -15 ^{o}C: (a) The separated hydrogels (CNCs-*g*-PPy 4.0 mg, PA 40.0 wt%) with different colors were brought into contact and healed without external stimulus. LED lights brightened when healed hydrogels were placed on the circuit. (b) The healed hydrogels could withstand stabs (c) The healed hydrogels could support 200.0 g weight. (d) Optical microscope images of hydrogels (CNCs-*g*-PPy 4.0 mg, PA 40.0 wt%) at -15 ^{o}C for various time.

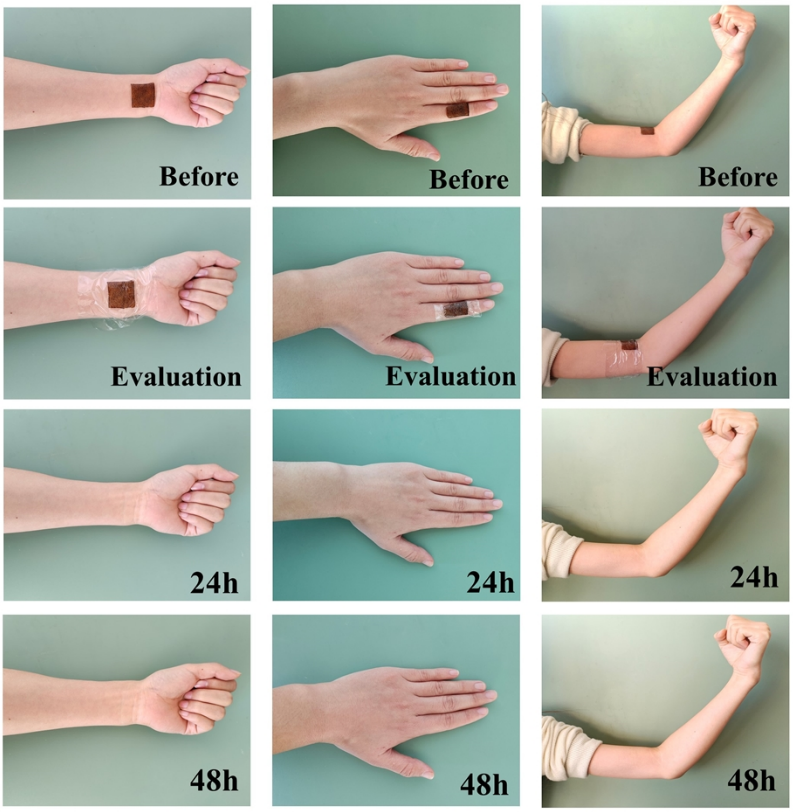

Fig. S8. The evaluation of skin irritation of human wrists, fingers and elbows by hydrogels.

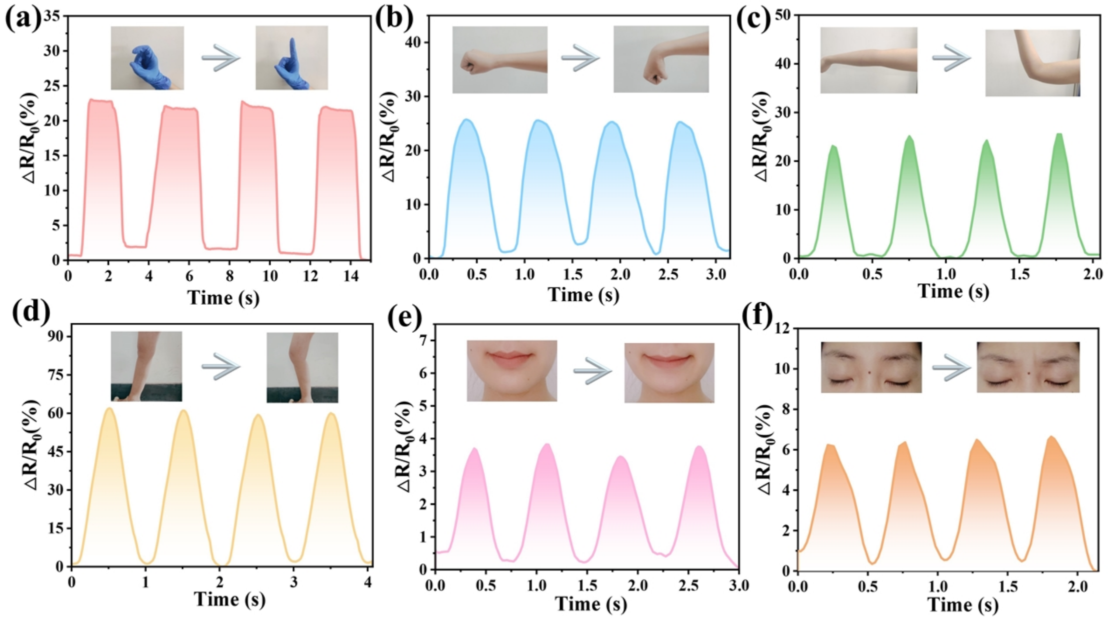

Fig. S9. Detection of human motion signals by hydrogel-based flexible sensors after freezing at -15 °C for 7 days: (a) fingers bending; (b) wrist bending; (c) elbow bending; (d) knee activity; (e)smile; (f) frown.

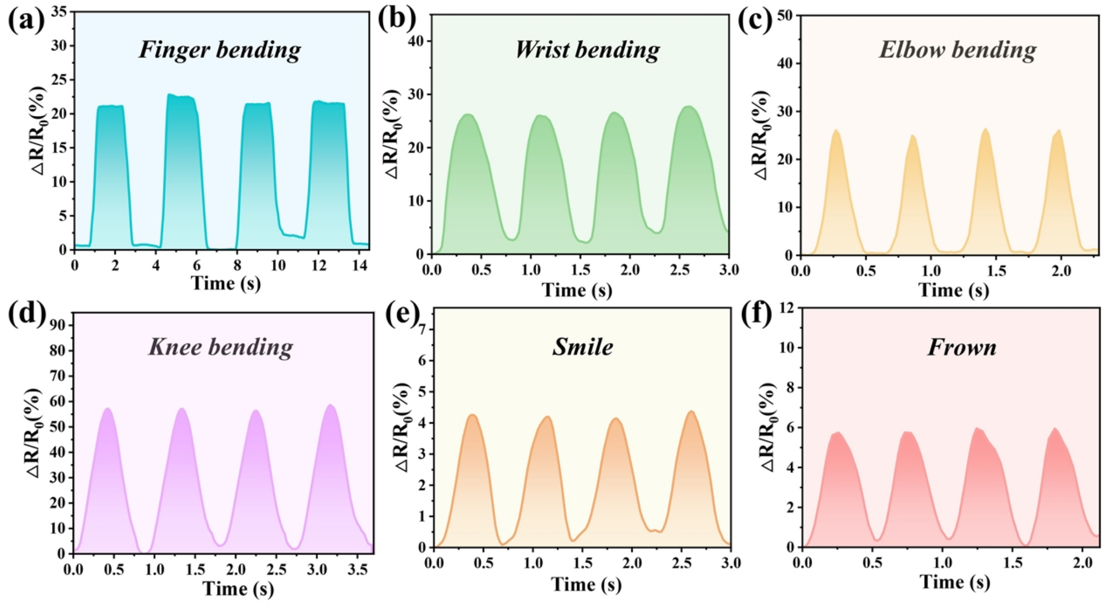

Fig. S10. Detection of human motion signals by hydrogel-based flexible sensors after self-healing: (a) fingers bending; (b) wrist bending; (c) elbow bending; (d) knee activity; (e)smile; (f) frown.

References

[S1] Y. T. Yang, H. Sun, C. H. Shi, Y. X. Liu, Y. C. Zhu and Y. M. Song, *Journal of Colloid and Interface Science*, 2023, **629**, 1021-1031.

[S2] C. Y. Lu, J. H. Qiu, W. Zhao, E. Sakai, G. H. Zhang, R. Nobe, M. Kudo and T. Komiyama, *International Journal of Biological Macromolecules*, 2021, **188**, 534-541.

[S3] X. F. Zhang, X. F. Ma, T. Hou, K. C. Guo, J. Y. Yin, Z. G. Wang, L. Shu, M. He and J. F. Yao, *Angewandte Chemie International Edition*, 2019, **58**, 7366-7370.

[S4] Y. P. Cheng, J. J. Zang, X. Zhao, H. Wang and Y. C. Hu, *Carbohydrate Polymers*, 2022, **277**, 118872.

[S5] Z. R. He and W. Z. Yuan, *ACS Applied Materials & Interfaces*, 2021, **13**, 1474-1485.

[S6] L. Bai, Y. Jin, X. Shang, H. Y. Jin, Y. T. Zhou and L. J. Shi, *Journal of Materials Chemistry A*, 2021, **9**, 23916-23928.

[S7] Q. C. Fan, Y. Nie, Q. Sun, W. X. Wang, L. J. Bai, H. Chen, L. X. Yang, H. W. Yang and D. L. Wei, *ACS Applied Polymer Materials*, 2022, **4**, 1626-1635.

[S8] L. He, D. Z. Ye, S. Weng and X. C. Jiang, *European Polymer Journal*, 2022, **181**, 111650.

[S9] L. Dong, M. X. Wang, J. J. Wu, C. Y. Zhang, J. Shi, K. Oh, L. R. Yao, C. H. Zhu and H. Morikawa, *Chemical Engineering Journal*, 2023, **457**, 141276.